NANO LETTERS

LETTER

pubs.acs.org/NanoLett

Capacitive Spring Softening in Single-Walled Carbon Nanotube Nanoelectromechanical Resonators

Chung Chiang Wu and Zhaohui Zhong*

Department of Electrical Engineering and Computer Science, University of Michigan, Ann Arbor, Michigan 48109, United States

Supporting Information

ABSTRACT: We report the capacitive spring softening effect observed in single-walled carbon nanotube (SWNT) nanoelectromechanical (NEM) resonators. The nanotube resonators adopt a dual-gate configuration with both bottom-gate and end-gate capable of tuning the resonance frequency through capacitive coupling. Interestingly, downward resonance frequency shifting is observed with increasing end-gate voltage, which can be attributed to the capacitive softening of the spring constant. Furthermore, in-plane vibrational modes exhibit a much stronger spring softening effect than out-of-plan modes. Our dual-gate design should enable the differentiation between these two types of vibrational modes and open up the new possibility for nonlinear operation of nanotube resonators.

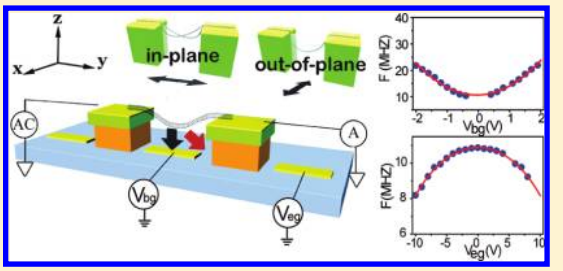

KEYWORDS: Single-walled carbon nanotube, NEMS, nanotube resonator, capacitive spring softening, elastic hardening

Because of their low mass density and high Young's modulus,[1−4] SWNTs offer great promise as ultrahigh frequency NEM resonators with applications in ultrasmall mass and force sensing.[5−10] To detect the mechanical vibration of nanotube resonators, various methods have been explored so far.[7,11−13] In particular, nanotube resonators can be actuated and detected simultaneously through electrostatic gate coupling, offering in situ frequency tuning over wide frequency range.[7,8] The gate-induced frequency tuning of NEM resonators is known to be governed by two mechanisms: the elastic hardening effect, which increases the resonance frequencies, and the capacitive softening effect, which decreases the resonance frequencies.[14−16] While the elastic hardening is originated from the increased beam tension, the capacitive softening is caused by beam oscillating in a constant electric field, which reduces the effective spring constant. Although elastic hardening effect has been widely reported in SWNT NEM resonators,[7,8,17] the field-induced capacitive spring softening has rarely been observed.[19] In a conventional nanotube resonator design,[7,13,17] only bottom-gate is used for frequency tuning. The nanotube vibrational motions[18,19] are perpendicular to the electric field direction, resulting in negligible spring softening. To this end, we demonstrate SWNT resonators with a dual-gate configuration, which enables both upward and downward frequency tuning by exploring elastic hardening and capacitive softening effects. Further, we discover that in-plane vibrational modes exhibit much stronger spring softening than out-of-plan mode, suggesting that the dual-gate technique can serve as an experimental method in differentiating vibrational modes.

SWNT NEM resonators with a dual-gate configuration are fabricated using the one-step direct transfer technique discussed previously.[20] Briefly, suspended SWNTs are grown across pillars on a transparent quartz substrate by the chemical vapor deposition (CVD) method,[21−23] while predesigned electrodes are fabricated on a separate device substrate by conventional lithography. The transfer of suspended SWNTs to the device substrate is implemented by simply bringing two substrates into contact. Figure 1a shows the scanning electron microscope (SEM) image of a typical dual-gate SWNT resonator. Suspended SWNT (indicated by the arrow) spans across the source (S) and drain (D) electrodes (in green) with an underneath bottom-gate (BG) and nearby end-gates (EG) electrostatically coupled to the nanotube. For a typical device, the S and D electrodes are 2 μm wide, separated by 3 μm, and the distance between nanotube and the BG is 1 μm. To explain how our dual-gate nanotube resonators can realize frequency-tuning through both elastic hardening and capacitive softening mechanisms, a qualitative sketch is illustrated in Figure 1b. SWNT resonators exhibit two types of vibration modes:[18,19] the in-plane mode (left-top panel) moves along the y-direction; and the out-of-plane mode (right-top panel), vibrating like a jumping rope, moves along the x-direction. When a voltage V_{bg} is applied on the BG electrode, the electrostatic force will pull down the nanotube toward the gate (gray arrow, along the z-direction), thus increasing the nanotube tension and resulting in elastic hardening. Since the electrostatic force is perpendicular to the vibration directions of both in-plane and out-of-plane modes, the effect of capacitive softening is negligible. On the other hand, when an end-gate voltage V_{eg} is applied, the electrostatic force (red arrow) will have component along y-direction in addition to z-direction. As the result, the in-plane vibrational modes will be impeded by the electrostatic force, leading to a strong capacitive softening effect compared to out-of-plane mode. Our dual-gate resonator design differs

Received: November 10, 2010
Revised: March 18, 2011
Published: March 23, 2011

ACS Publications © 2011 American Chemical Society

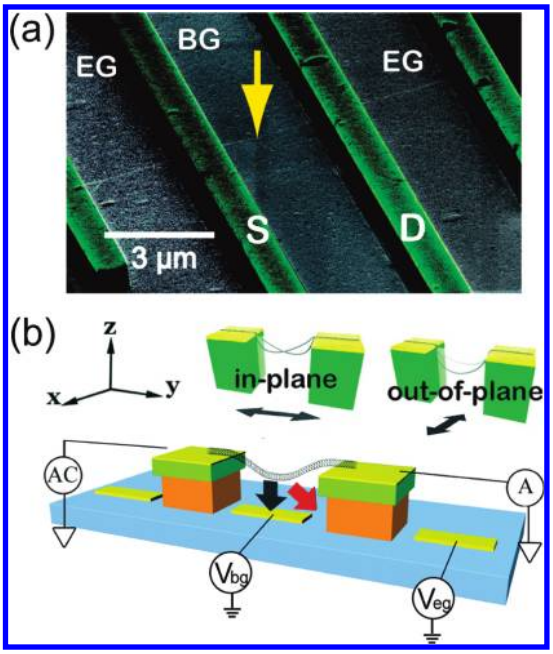

Figure 1. Device geometry of dual-gate SWNT resonators. (a) The SEM image of SWNT NEM resonators. The source and drain electrodes are colorized (green) and 50 nm thick Au is used as the bottom-contact metal. The arrow indicates the position of a suspended SWNT. (b) A qualitative sketch illustrates how electrostatic force interacts with different resonance modes when a bias voltage is applied on BG or EG electrodes.

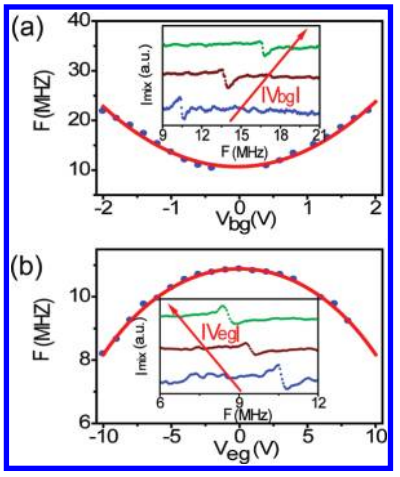

Figure 2. Resonance characteristics of a dual-gate SWNT resonator. (a) Elastic hardening effect, and (b) capacitive softening effect, observed on a SWNT NEM resonator by biasing BG and EG, respectively. The single-source mixing technique is used for resonance actuation and detection with δV_{sd} = 10 mV, and measurement is done in a vacuum chamber at pressure below 10^{-4} Torr. Insets of (a,b): mixing current (I_{mix}) vs driving frequency (f) at different BG and EG voltages. Resonance peak shifts to higher frequency as $|V_{bg}|$ = 0.5, 1, and 1.5 V is applied, and shift to lower frequency as $|V_{eg}|$ = 3, 7, and 9 V is applied.

from previous work,[15] where the second gate electrode (side-gate) is also perpendicular to the resonator beam. The adoption of end-gate design drastically reduces the fabrication complexity and enhances the softening effect for the in-plane vibrational modes.

To experimentally examine these two frequency tuning mechanisms, we systematically applied voltages on both bottom-gate and end-gate electrodes. A small AC driving voltage of 10 mV applied to the drain electrode was used to actuate the resonator through electrostatic interaction, and resonance frequency was detected by measuring the frequency-dependent mixing current I_{mix} described in previous literatures.[7,8] We first studied the frequency tuning using bottom-gate electrode. As shown in Figure 2a inset, nanotube resonances are clearly visible, and resonance frequency increases from 11 to 22 MHz as $|V_{bg}|$ increases from 0 to 2 V. We further extract resonance frequencies at different V_{bg} between −2 to 2 V, and the results can be fitted with a parabolic function (Figure 2a). Our observation of frequency tuning using BG electrode agrees well with elastic hardening effect reported on nanotube resonators.[7,17] At small BG voltage, the nanotube resonators operate in the bending regime,[7,17−19] in which resonance frequency f depends quadratically on the BG voltage[3,18,19]

$$f = f_0 + 0.28\frac{C'}{\sqrt{96s}}\sqrt{\frac{1}{\mu EI}}V_{bg}^2 = f_0 + AV_{bg}^2 \qquad (1)$$

where f_0 is the fundamental frequency, C' is the first derivative of capacitance to nanotube/gate distance, s is the slack, μ is linear mass density, E is Young's modulus, I is the moment of inertia, and A is termed as elastic hardening tuning coefficient. Fitting the experimental data in Figure 2a with eq 1 yields measured coefficient A of 1.9×10^6 Hz V^{-2}. To compare A with the theoretical value A_{theory}, we adopted a cylinder over a metal plane to model the capacitance $C = (2\pi\varepsilon_0 L)/(\ln(2Z/d))$, where ε_0 is the dielectric constant; L is the nanotube length; Z is the separation between tube and bottom electrode; and d is the diameter of the nanotube. Assuming a small slack of 1% and typical SWNT parameters,[18] listed in Table S1 of the Supporting Information, the A_{theory} value calculated using eq 1 is 2.5×10^6 Hz V^{-2}, which agrees well with measured A.

Next, we examined the frequency dependence of end-gate voltage (Figure 2b). Interestingly, as shown in Figure 2b inset, nanotube resonance frequency decreases as $|V_{eg}|$ increases. The extracted resonance frequencies at different V_{eg} between −10 to 10 V exhibit a negative curvature with increasing field. The observed downward frequency tuning by EG is in strong contrast to elastic hardening, but it can be explained by the capacitive softening effect. The frequency dependence of the capacitive softening effect can be expressed as[14,15]

$$f^2 = f_0^2 - \frac{C''V_{eg}^2}{8\mu L\pi^2} = f_0^2 - BV_{eg}^2 \qquad (2)$$

where C'' is the second derivative of capacitance, and B is termed the capacitive softening coefficient. Again, fitting the experimental data in Figure 2b with eq 2 yields the measured coefficient B of 0.8×10^{12} Hz^2 V^{-2}. To calculate the theoretical value of B_{theory}, a finite-element simulation (COMSOL) is performed to obtain C'' for EG (Supporting Information Figure S2). Using typical SWNT parameters of Supporting Information Table S1 and C'' obtained from simulation, we calculate a B_{theory} from eq 2 of 0.96×10^{12} Hz^2 V^{-2}, which agrees with measured B. Similar results have been observed on three dual-gate resonators, offering a reliable approach for studying both elastic hardening and capacitive softening effects in nanotube resonators for the first time.

SWNT resonators are known to exhibit multiple vibrational states, including in-plane, out-of-plane, and their higher order

dx.doi.org/10.1021/nl1039549 |Nano Lett. 2011, 11, 1448–1451

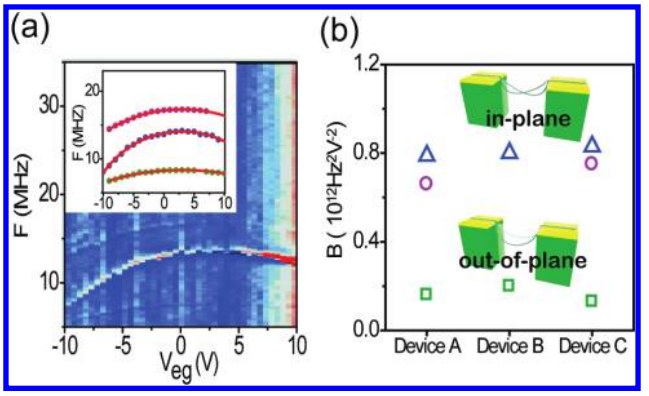

Figure 3. Capacitive spring softening effect observed on different vibrational modes. (a) Mixing current I_{mix} (color scale) is plotted as a function of driving frequency and V_{eg}. Inset: Resonance peaks (blue dots) of different modes are plotted with respect to V_{eg}. Red lines are fitting curves with eq 3. (b) Measured softening coefficients (Bs') of different modes for three resonators. The softening coefficients for the first vibration modes (green squares) are always much smaller than those of higher order modes (blue triangles and purple circles), differed by 4 to 6.3 times.

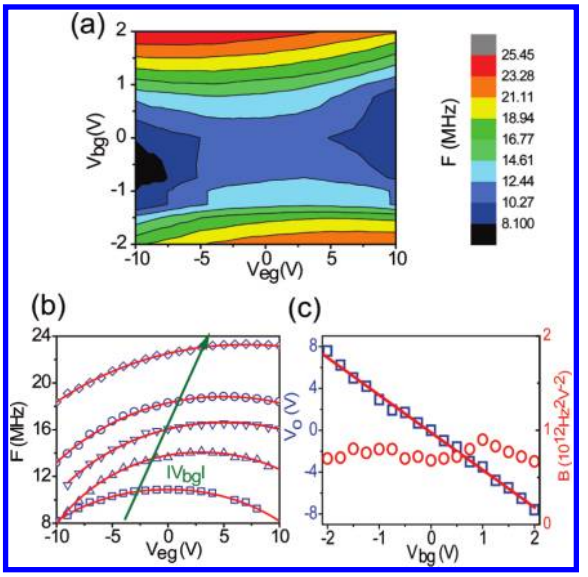

Figure 4. Dual-gate frequency tuning of SWNT resonator. (a) Two-dimensional plot of resonance frequency (in color) vs V_{sg} and V_{eg} for the second vibrational mode. (b) Resonance frequencies (blue dots) vs V_{eg} curves for V_{bg} = 0, −1, −1.25, −1.5, and −2 V, from bottom to top. The neutral point V_0 shifts to higher voltages as $|V_{bg}|$ increases. (d) Offset voltage V_0 (blue squares) and coefficient B (red circles) vs V_{bg} extracted from (c). A linear fit of V_0 vs V_{bg} yields a slope of ∼3.

modes.[18,19] We therefore examined the capacitive softening effect for different vibrational modes. Figure 3a shows the mixing current (in color) plotted as a function of driving frequency and EG voltage. Three resonance modes are clearly visible with f up to 23 MHz, and they all exhibit capacitive softening effect with applied V_{eg}. The V_{eg}-dependent resonance frequencies for all three modes are plotted in the inset of Figure 3a. Importantly, three vibrational modes show drastically different tunability. Fitting the experimental data in Figure 3a inset with eq 2 yields B = 0.16, 0.8, and 0.76 × 10^{12} Hz^2 V^{-2} for vibrational modes from bottom to top, respectively. The two higher frequency modes exhibit ∼5 times larger capacitive softening effect compared to the lowest frequency mode. Similar measurements were performed on 3 other SWNT resonators with the same device geometry, and the results are shown in Figure 3b. The softening coefficients for the first vibration modes are always much smaller than those of higher order modes, differed by 4 to 6.3 times. This observation agrees with our qualitative analysis shown in Figure 1b, where differences in softening coefficients are expected for in-plane and out-of-plane modes. Therefore, we attribute the first vibrational mode with much smaller softening coefficient as out-of-plane mode, and the higher order vibrational modes with larger softening coefficients as in-plane modes. Our results also agree with the theoretical prediction of the first vibrational mode being the fundamental out-of-plane mode.[18,19]

Last, we investigated how the coupling of BG and EG affects the capacitive softening effect. A two-dimensional (2D) plot of resonance frequency (in color) versus V_{sg} and V_{eg} for the second vibrational mode is shown in Figure 4a. The resonance frequencies show symmetric tuning around gate voltages corresponding to the charge neutral point, although a shift of neutral point is clearly observed. Furthermore, the V_{eg}-dependent resonance frequencies for different fixed V_{bg} are plotted in Figure 4b. As $|V_{bg}|$ increases from 0 to 2 V, the downward frequency tuning is again clearly visible, but the curves are shifted toward higher V_{eg} value. The shift rises from our dual-gate geometry, where the charge neutral point will shift as voltage being applied onto the EG. The capacitive softening equation can be modified by including the effect of elastic hardening and an offset voltage, V_0, to account for the effect of BG

$$f^2 = f_0'^2 - B(V_{eg} - V_0)^2 = (f_0 + AV_{bg}^2)^2 - B(V_{eg} - V_0)^2 \quad (3)$$

Fitting data in Figure 4c with eq 3, we extracted the softening coefficient B and offset voltage V_0, and the results are plotted in Figure 4c. The softening coefficient (red circles) remains nearly constant at different V_{bg} voltage, while V_0 (blue squares) varies linearly with respect to V_{bg}. A linear fit of V_0 versus V_{bg} yields a slope of ∼3, suggesting that the BG is about three times more effective than EG for electrostatic charging. We note that DC conductance versus V_{bg} and V_{eg} plot (Supporting Information Figure S1) reveals ∼10 times stronger BG coupling compared to EG. This discrepancy between the DC conductance measurement and the resonance frequency shifting measurement is not understood at present time, and requires further investigation.

In summary, we report the observation of capacitive softening effect in SWNT NEM resonators with dual-gate configuration. While in-plane vibrational modes show strong softening effect when EG voltage is applied, the fundamental out-of-plan mode exhibits small/negligible spring constant softening. Our results not only provide a new experimental tool for differentiating nanotube vibrational modes but also enable additional freedom for exploring nonlinear effects in nanotube resonators. The quality factors of our nanotube resonators range from 30 to 150 at room temperature, which are consistent with the literatures.[7,20] The capability of spring constant tuning by EG coupling enables parametric nanomechanical amplification for quality factor enhancement,[24] and makes possible nanotube resonator-based room temperature single molecule mass sensor.

dx.doi.org/10.1021/nl1039549 |*Nano Lett.* 2011, 11, 1448–1451

■ ASSOCIATED CONTENT

Supporting Information. Additional table and figures. This material is available free of charge via the Internet at http://pubs.acs.org.

■ AUTHOR INFORMATION

Corresponding Author
*E-mail: zzhong@umich.edu.

■ ACKNOWLEDGMENT

The work is supported by the startup fund provided by the University of Michigan. This work used the Lurie Nanofabrication Facility at University of Michigan, a member of the National Nanotechnology Infrastructure Network funded by the National Science Foundation.

■ REFERENCES

(1) Lu, J. P. *Phys. Rev. Lett.* **1997**, *79*, 1297–1300.
(2) Krishnan, A.; Dujardin, E.; Ebbesen, T. W.; Yianilos, P. N.; Treacy, M. M. J. *Phys. Rev. B* **1998**, *58*, 14013–14019.
(3) Sapmaz, S.; Blanter, Y. M.; Gurevich, L.; van der Zant, H. S. J. *Phys. Rev. B* **2003**, *67*, 235414.
(4) Hierold, C.; Jungen, A.; Stampfer, C.; Helbling, T. *Sens. Actuators A* **2007**, *136*, 51–61.
(5) Cleland, A. N. *Foundations of Nanomechanics*; Springer-Verlag: Berlin, 2003.
(6) Kis, A.; Zettl, A. *Philos. Trans. R. Soc. London, Ser. A* **2008**, *366*, 1591–1611.
(7) Sazonova, V.; Yaish, Y.; Ustunel, H.; Roundy, D.; Arias, T. A.; McEuen, P. L. *Nature* **2004**, *431*, 284–287.
(8) Peng, H. B.; Chang, C. W.; Aloni, S.; Yuzvinsky, T. D.; Zettl, A. *Phys. Rev. Lett.* **2006**, *97*, 087203.
(9) Lassagne, B.; Garcia-Sanchez, D.; Aguasca, A.; Bachtold, A. *Nano Lett.* **2008**, *8*, 3735–3738.
(10) Chiu, H. Y.; Hung, P.; Postma, H. W. C.; Bockrath, M. *Nano Lett.* **2008**, *8*, 4342–4346.
(11) Babic, B.; Furer, J.; Sahoo, S.; Farhangfar, S.; Schonenberger, C. *Nano Lett.* **2003**, *3*, 1577–1580.
(12) Garcia-Sanchez, D.; Paulo, A. S.; Esplandiu, M. J.; Perez-Murano, F.; Forro, L.; Aguasca, A.; Bachtold, A. *Phys. Rev. Lett.* **2007**, *99*, 085501.
(13) Steele, G. A.; Huttel, A. K.; Witkamp, B.; Poot, M.; Meerwaldt, H. B.; Kouwenhoven, L. P.; van der Zant, H. S. J. *Science* **2009**, *325*, 1103–1107.
(14) Kozinsky, I.; Postma, H. W. C.; Bargatin, I.; Roukes, M. L. *Appl. Phys. Lett.* **2006**, *88*, 253101.
(15) Fung, W. Y.; Dattoli, E. N.; Lu, W. *Appl. Phys. Lett.* **2009**, *94*, 203104.
(16) Unterreithmeier, Q. P.; Weig, E. M.; Kotthaus, J. P. *Nature* **2009**, *458*, 1001–1004.
(17) Witkamp, B.; Poot, M.; van der Zant, H. S. J. *Nano Lett.* **2006**, *6*, 2904–2908.
(18) Sazonova, V. *A Tunable Carbon Nanotube Resonator*. PhD. Thesis, Cornell University, Ithaca, NY, 2006.
(19) Ustunel, H.; Roundy, D.; Arias, T. A. *Nano Lett.* **2005**, *5*, 523–526.
(20) Wu, C. C.; Liu, C. H.; Zhong, Z. *Nano Lett.* **2010**, *10*, 1032–1036.
(21) Dresselhaus, M. D.; Dresselhaus, G.; Avouris, Ph. *Carbon Nanotubes: Synthesis, Structure Properties and Applications*. Springer-Verlag: Berlin, 2001.
(22) Kong, J.; Soh, H. T.; Cassell, A. M.; Quate, C. F.; Dai, H. J. *Nature* **1998**, *395*, 878–881.
(23) Zhang, Y. Y.; Zhang, Y.; Xian, X. J.; Zhang, J.; Liu, Z. F. *J. Phys. Chem. C* **2008**, *112*, 3849–3856.
(24) Karabalin, R. B.; Feng, X. L.; Roukes, M. L. *Nano Lett.* **2009**, *9*, 3116–3123.